

# Aging in the transport on the corrugated ratchet potential

Karina I. Mazzitello<sup>1</sup>, Daniel G Zarlenga<sup>1</sup>, Fereydoon Family<sup>2</sup>,  
Constancio M Arizmendi<sup>1</sup>

<sup>1</sup> Instituto de Investigaciones Científicas y Tecnológicas en Electrónica,  
Universidad Nacional de Mar del Plata, B7608 Mar del Plata, Buenos Aires,  
Argentina

<sup>2</sup> Department of Physics, Emory University, Atlanta, GA 30322, USA

E-mail: <sup>1</sup> kmazzite@mdp.edu.ar

**Abstract.** Under rapid undercooling, glass forming liquids freeze in an amorphous state that can equilibrate only on enormously long time-scales. This is the characteristic sign of aging, which has been observed in a wide range of systems. Brownian ratchet is a widely studied system that exhibits many types of anomalous dynamical behavior. We have investigated the possibility of aging in the collective motion of Brownian particles in a periodic ratchet potential with quenched disorder. We find that when a slowly growing fraction of particles are trapped for long time, the collective movement tends to become super-diffusive. The super-diffusive transport weakly breaks the ergodicity and the time to cover the whole phase space become enormously long and reminiscent of aging behavior.

*Keywords:* anomalous transport, aging, ratchet potential, quenched correlated disorder

## 1. Introduction

Disorder in stochastic systems may lead to anomalous behaviors characterized by significant variations of the observed properties, for finite time scales. These variations produce systematic deviations of the dynamical property mean value which are usually much larger than statistical errors. A particular class of systems where anomalous behaviors of this type occur are the so-called glass-forming systems. These systems include, for example, disordered spin systems close to the spin-glass transition [1], supercooled molecular liquids [2, 3] and jamming colloidal solutions [4]. The physics of a glass-forming liquid is such that when rapidly undercooled under its melting temperature, it loses its ability to flow on experimental time-scales. Glassy materials freeze in an amorphous state that requires enormously long time to equilibrate [5, 6]. This is the characteristic sign of aging, where systems whose properties depend on the age of the system can be quantified through the so-called relaxation or waiting time.

Relaxation times are proportional to the viscosity of the glass and that is why they grow with increasing fluid viscosity.

Recently [7, 8, 9], aging phenomena were studied in several physical systems that involve anomalous dynamics associated with spatial disorder and ratchet potentials. One of these physical systems is a colloidal gel [7]. In the coarsening and age-related changes of an aging colloidal gel, Zia *et al.* [7] found that the gel strands contain a glassy, immobile interior near random-close packing, surrounded by a liquidlike surface coarsened by the diffusive migration of particles. This coarsening is a three-step process: cage formation, where particles travel rapidly along the network surface until they become bonded to neighbors, cage hopping, characterized by migration of particles between cages, and finally cage trapping where particles get buried within network strands. The motion of the particles is stochastic, but with a net drift to a less-mobile and higher contact number states. Zia *et al.* [7] characterize the dynamics as the motion of the particles in a ratchet potential resulting from coarsening and aging. In addition to the work of Zia *et al.* [7], Chadhuri *et al.* [8] have made large-scale simulations of aging gels. They also find anomalous behavior in the form of subdiffusive caged dynamics crossing over to large length scale superdiffusive particle motion associated with heterogeneities.

Another important example of aging phenomena is exhibited in the dynamics of magnetic skyrmions [9] through anomalous behaviors produced by disorder and ratchet motion. Skyrmions are nanometer size, particle-like spin textures present in certain chiral magnets, with enforced stability due to their integer topological charge [9]. Skyrmions are often considered to be candidates for bits in racetrack data storage devices that may replace typical RAM or HDD memories [10] in the near future. The skyrmions advantage over typical ferromagnetic domain walls is because racetrack operates purely electrically and skyrmions can be driven by very low current densities [11]. The mobility of skyrmions is affected by defects in magnetic materials, such as vacancies [12], or magnetic grains with varying anisotropy [13, 14]. Consequently, skyrmions can undergo pinning due to these magnetic defects. Thus, there exists a depinning threshold for skyrmion motion in the presence of defect induced disorder that leads to different types of flow and transitions between different phases [15, 16]. Defects also produce anomalous dynamics and aging in skyrmions [17, 18].

In connection with the study of anomalous diffusion, several models have revealed a behavior reminiscent of aging [19, 20]. Khoury *et al.* [19] found strong fluctuations in the usual ensemble calculation of the diffusion coefficient in the overdamped motion of particles in a tilted washboard potential, indicating that the system exhibits aging. In [20], the authors have analyzed properties like ergodicity breaking and nonstationarity in the transient motion of inertial particles in a ratchet potential. In this work, we establish a relationship between anomalous diffusion associated with defects, ratchet motion, and aging in a model of corrugated ratchet potential, recently introduced in [20, 21]. Up to our knowledge, this is the first time in which aging is quantified and is related to particle diffusion in a simple ratchet model.

The outline of the paper is as follows. We provide a detailed description of the model and its associated dynamical equations, in section 2. A brief analysis of the magnitudes of the quenched disorder is presented in the same section. The different categories of diffusion characterized by the mean-square displacement and their relations to the mean velocity of the particles is discussed in section 3.1. The aging of the transport on the corrugated ratchet potential is studied in section 3.2. This property is revealed by measuring the velocity correlation of the system that depends on two times. The same type of dependence is also found in correlation functions of real glasses [19, 20]. Finally, section 4 consists of concluding remarks.

## 2. Model and simulation method

The model is defined by considering the overdamped motion of identical non-interacting Brownian particles in a rocking ratchet potential with a quenched disorder [21]. The stochastic differential equation (Langevin equation) for such particles is given by

$$\gamma \dot{x} = F_0 \sin(\omega t) + \xi(t) - dU(x)/dx, \quad (1)$$

where the left-hand side describes a frictional force experienced by the particles when they move relative to their environment, with  $\gamma$  being the drag coefficient. The first term of the right-hand side is an external sinusoidal force with a frequency  $\omega$  and amplitude  $F_0$  that pushes the particles left and right periodically (rocking ratchet). The second term is Gaussian thermal noise at temperature  $T$ . The correlation function of the noise obeys the fluctuation-dissipation relation  $\langle \xi(t)\xi(t') \rangle = 2\gamma k_B T \delta(t - t')$ . Ultimately, the last term of the right-hand side in Eq. (1) is the force due to the ratchet potential  $V_p(x)$  and the quenched spatial disorder  $V_r(x)$ . They contribute to the total potential  $U(x)$  through the parameter  $\sigma = [0, 1]$  according to

$$U(x) = (1 - \sigma) V_p(x) + \sigma V_r(x). \quad (2)$$

Here  $V_p(x)$  is the archetypal ratchet potential of double-sine [22]

$$V_p(x) = -V_0 [\sin(2\pi x/\lambda_p) + (\mu/2) \sin(4\pi x/\lambda_p)], \quad (3)$$

where  $V_0$ ,  $\lambda_p$  and  $\mu = [0, 0.5]$  are the amplitude, the spatial period and the asymmetry, respectively and  $V_r(x)$  is a Gaussian spatially random contribution with correlation function

$$g_r(x) = \langle V_r(x)V_r(0) \rangle = g_0 \exp(-2\pi^2 x^2/l_r^2), \quad (4)$$

where  $g_0$  is the amplitude and  $l_r$  is the ratchet potential roughness. Indeed, smaller values of  $l_r$  lead to a greater number and height of the barriers on the potential  $V_p(x)$ .

In addition, in order to ensure that the amplitude of the total potential is of the order of  $V_0$  independently of  $\sigma$ , we choose correlations of both ratchet and random potentials to be the same at  $x = 0$ . The correlation function for the ratchet potential is

$$g_p(x) = V_0^2/2 [\cos(2\pi x/\lambda_p) + (\mu/2)^2 \cos(4\pi x/\lambda_p)] \quad (5)$$

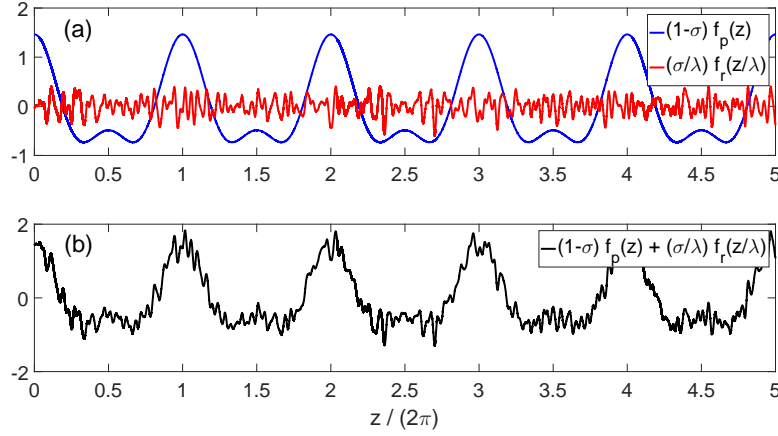


**Figure 1.** (a) Relative contributions of a realization of the quenched - disorder force and of the ratchet force, for  $\sigma = 0.025$ ,  $\lambda = 0.095$ ,  $\mu = 0.5$ ,  $\tilde{F}_0 = 1.47$ ,  $\Omega = 0.1$  and  $\lambda_p = 2\pi$ . (b) Resulting force sum of the quenched disorder force and the ratchet force (see Eq. (6)). The disorder level is indeed perceptible for these parameter values.

Thus, from Eqs. (4) and (5) and matching  $g_r(0) = g_p(0)$ , the amplitude of the correlation function (4) is  $g_0 = 17V_0^2/32$ .

The equation of motion (1) can be reduced into a dimensionless form in terms of the rescaled spatial and temporal quantities  $z = 2\pi x/\lambda_p$  and  $\tau = [(2\pi)^2 V_0/\gamma\lambda_p^2] t$  as [23]

$$\dot{z} = -(1-\sigma)f_p(z) - (\sigma/\lambda)f_r(z/\lambda) + \tilde{F}_0 \sin(\Omega\tau) + \eta(\tau), \quad (6)$$

where  $f_p$  and  $f_r$  are the dimensionless forces arising from the ratchet  $V_p$  and random  $V_r$  potentials, respectively,  $\Omega$  and  $\tilde{F}_0$  are the frequency and amplitude of the applied dimensionless sinusoidal force, and  $\eta(\tau)$  is the dimensionless noise. The dimensionless parameters

$$\lambda = \frac{l_r}{\lambda_p}, \quad \tilde{F}_0 = F_0 \frac{\lambda_p}{2\pi V_0}, \quad \text{and} \quad \tilde{T} = \frac{k_B T}{V_0} \quad (7)$$

combined with  $\sigma = [0, 1]$  and  $\Omega = \omega \frac{\gamma\lambda_p^2}{(2\pi)^2 V_0}$  define the motion of particles subject to Eq. (6). By using Eqs. (7), the dimensionless noise correlation function is  $\langle \eta(\tau)\eta(\tau') \rangle = 2\tilde{T}\delta(\tau - \tau')$ .

In Fig. 1(a), an example of the disorder contributing to the ratchet force is shown, already weighted with the parameters  $\sigma = 0.025$  and  $\lambda = 0.095$ , according to Eq. (6) and for  $\mu = 0.5$ ,  $\tilde{F}_0 = 1.47$ ,  $\Omega = 0.1$  and  $\lambda_p = 2\pi$ . A decrease of  $\lambda$  even for fixed  $\sigma$  leads to an increase in the relative contribution of the random force. Adding this disorder to the contribution of the ratchet force results in a disorder level perceptible in the scale of the total force (part (b) of Fig. 1).

Throughout this work we set  $\sigma = 0.025$  and  $\lambda = 0.095$ , associated with a rough total force like that shown in Fig. 1(b). As we shall see in the next section, increasing  $\lambda$  diminishes the effects of the disorder and loses variants of anomalous transport. In

addition,  $\Omega$  and  $\lambda_p$  are also set to 0.1 and  $2\pi$ , respectively. Variations in  $\Omega$  do not lead to any additional phenomenology, while the specific choice of  $\lambda_p$  is only important as a reference value.

We have carried out numerical simulations of the Eq. (6) over a large number ( $10^3 - 10^4$ ) of particle trajectories. Each particle moves in a different random potential starting at  $z = 0$ . The method to generate the random force values is described in [24] in more detail. In order to characterize the transport, we measured the diffusion coefficient  $D$  and the mean velocity  $\langle v \rangle$  of the particles, which are given by

$$\begin{aligned} D(\tau) &= \frac{\langle (z(\tau) - \langle z(\tau) \rangle)^2 \rangle}{2\tau}, \\ \langle v(\tau) \rangle &= \frac{\langle z(\tau + \Delta\tau) - z(\tau) \rangle}{\Delta\tau}, \end{aligned} \quad (8)$$

where  $\langle \dots \rangle$  indicates the average taken over the many trajectories and  $\Delta\tau$  is chosen equal to  $2\pi/\Omega$  (see next section). We also computed the two-time velocity correlation

$$C_v(\tau, \tau_w) = \frac{\langle v(\tau)v(\tau_w) \rangle - \langle v(\tau) \rangle \langle v(\tau_w) \rangle}{\langle v(\tau_w)^2 \rangle - \langle v(\tau_w) \rangle^2} \quad (9)$$

to analyze the ergodicity breaking, with  $\tau \geq \tau_w$ . Note that, the velocity correlation  $C_v(\tau, \tau_w) = 1$ , for  $\tau = \tau_w$ , and it decreases as  $\tau$  moves away from  $\tau_w$ .

### 3. Results and Discussion

#### 3.1. Anomalous transport

The quenched noise can have two kinds of effects on diffusion properties: It may only affect the value of the transport coefficients (velocity, diffusion constant, etc.) as compared to the ordered system or it may alter in various ways the diffusion behavior [25]. We are mainly concerned here with anomalous diffusion phenomena, where the second kind of effect takes place. The first effect occurs when the external force amplitude is less than the amplitude of the ratchet in which case, due to the quenched disorder, a transient subdiffusive behavior is found and then the particles achieve a constant mean velocity with normal diffusion. The second kind of effect is obtained when the external force amplitude is greater than the amplitude of the ratchet in which case a variety of anomalous behaviors are obtained. Subdiffusive and superdiffusive transports are shown in Fig. 2(a) and (b), respectively, in which  $D$  is plotted versus  $\tau$  for  $\mu = 0.1$ ,  $\lambda = 0.095$ ,  $\tilde{F}_0 = 1.47$  at different temperatures. The black curve in part (a), corresponds to  $\tilde{T} = 0$ , in which, after a superdiffusive transient all the particles are stopped due to the barriers imposed by the quenched disorder [24]. Without thermal noise, the movement has just a transient nature. In contrast, as  $\tilde{T}$  increases, anomalous diffusion is reached at long times with  $D$  scaling with time as  $D(\tau) \sim \tau^\beta$ , where the exponent  $\beta$  characterizes the different regimes observed:  $-1 < \beta < 0$  corresponds to subdiffusion,  $\beta > 0$  to superdiffusion and  $\beta = 0$  to normal diffusion. The exponent  $\beta$  for different temperatures is shown

in the fourth column of table 1. The motion tends to be subdiffusive at low temperatures, superdiffusive at intermediate temperatures and Brownian at high temperatures. The different regimes are related to how the particles explore the landscape. As we shall see in section 3.2, at low temperatures, most of the particles explore every landscape detail and the movement is subdiffusive. The thermal noise makes the particles jump over many disorder potential peaks and less particles are trapped. In this case, the collective movement tends to disperse and it is superdiffusive. Finally, normal diffusion appears when high enough temperatures dominate particles motion. **Indeed, increasing the temperature, the particles can sort the quenched disorder more easily and thus, the movement tends to disperse less with a higher mean velocity, as will be seen below.**

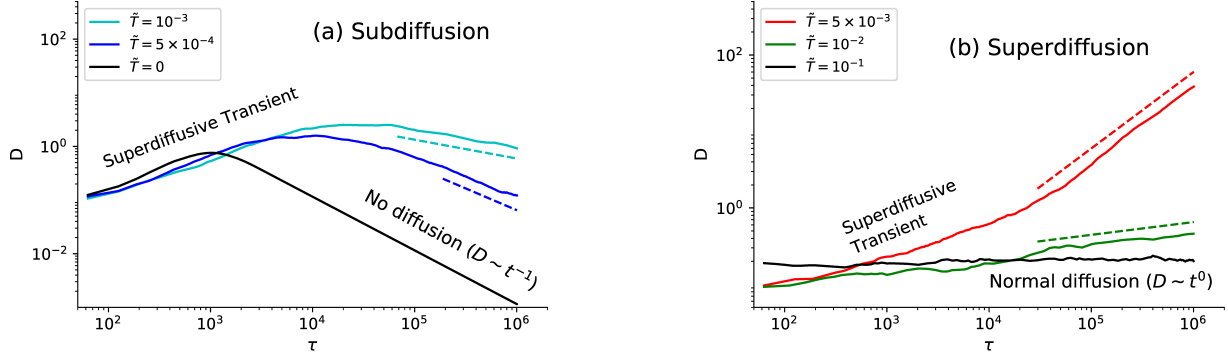


**Figure 2.** Log-log plots of the diffusion coefficient versus the rescaled time, corresponding to different choices of the dimensionless temperature  $\tilde{T}$  as indicated and for fixed external force amplitude  $\tilde{F}_0 = 1.47$ , quenched noise correlation length  $\lambda = 0.095$  and ratchet potential asymmetry  $\mu = 0.1$ . (a) Subdiffusive behaviors and a no diffusive case. (b) Superdiffusive behaviors and a diffusive case. Dashed lines correspond to the asymptotic behavior and their slopes are stored in the fourth column of table 1.

The spatial disorder slows down the particle collective motion and the mean velocity decreases over time (subtransport) or at most, it can be constant. This is clearly observed in Fig. 3, where we show the mean velocity as a function of  $\tau$ , for the same values of thermal noise as those corresponding to the previous figure. The mean velocity is constant or tends to decrease as  $\langle v \rangle \sim \tau^{-\alpha}$ , with  $\alpha > 0$  and for  $\tau \gg 1$ .

Following the reasoning in [23] applied to anomalous diffusion, we establish a relation between the exponents  $\alpha$  and  $\beta$  of the velocity and the diffusion coefficient, respectively. As mentioned previously, the quenched noise can alter the very elementary properties of Brownian motion. For Brownian motion,  $D$  is a constant given by

$$D(\tau) = \frac{\lambda_p^2 [\langle \tau_p^2 \rangle - \langle \tau_p \rangle^2]}{2 \langle \tau_p \rangle^3} \quad (10)$$

**Table 1.** Exponents  $\alpha$  and  $\beta$  for different values of the temperature and for fixed external force amplitude  $\tilde{F}_0 = 1.47$  and correlation length of quenched noise  $\lambda = 0.095$ .  $\alpha$  is obtained from asymptotic values of the slope of  $\log(v)$  versus  $\log(\tau)$  (third column see Fig. 3), while  $\beta$  is obtained in two different ways: from asymptotic values of the slope of  $\log(D)$  versus  $\log(\tau)$  (fourth column see Fig. 2) and from Eq.(11) (fifth column).

$\mu$	$\tilde{T}$	$\alpha$	$\beta$	$\beta^*$
0.1	$5 \times 10^{-4}$	0.86	-0.74	-0.72
	$10^{-3}$	0.71	-0.33	-0.42
	$5 \times 10^{-3}$	0.05	1.00	0.90
	$10^{-2}$	0.00	0.17	—
	$10^{-1}$	0.00	1.00	—
0.5	$3 \times 10^{-4}$	0.81	-0.66	-0.62
	$10^{-3}$	0.00	1.27	—

\* valid for  $\alpha > 0$  (see before Eq.(11), in the main text).

provided the first two moments  $\langle \tau_p \rangle$  and  $\langle \tau_p^2 \rangle$  of the distribution  $P(\tau_p)$  are finite, where  $\tau_p$  is the time that it takes a single particle to cover the spatial period of the ratchet potential  $\lambda_p$  over the course of its trajectory for long enough time. In contrast, when any of the first two moments of  $P(\tau_p)$  diverges, anomalous diffusion can be obtained.

According to our numerical results, the asymptotic behavior of the mean velocity can be calculated from Eq. (8), as  $\langle v \rangle = \langle z \rangle / \tau$  or also as  $\langle v \rangle = \lambda_p / \langle \tau_p \rangle$ . When the velocity decays as  $\langle v \rangle \sim \tau^{-\alpha}$ ,  $\langle \tau_p \rangle$  varies as  $\tau^\alpha$  and therefore the distribution  $P(\tau_p)$  has a tail that decreases as a power-law for long stretches of time [23]. In this regime,  $\langle \tau_p^2 \rangle \sim \tau^{\alpha+1}$  and from Eq. (10), we find

$$\beta = 1 - 2\alpha, \quad (11)$$

for  $\tau \gg 1$ . When  $0 < \alpha < 1/2$ , the movement of the particles is superdiffusive and when  $1/2 < \alpha < 1$  the movement is subdiffusive. The values of  $\beta$  obtained from Eq. (11) are listed in the 5th column of Table 1. These values are consistent with the slopes obtained from Fig. 2 (4th column of table 1) except for  $\mu = 0.1$  and  $\tilde{T} = 10^{-3}$  where needs much more time to reach the asymptotic behavior.

Finally, when the mean velocity is constant,  $\langle \tau_p \rangle = \lambda_p / \langle v \rangle$  is finite and  $\langle \tau_p^2 \rangle$  can be finite or diverge over time. In this case, the movement of particles is Brownian or superdiffusive (see the black and the green graphs in Figs. 2(b) and 3).

In summary, when  $P(\tau_p)$  decreases as a power-law, anomalous diffusion with asymptotic behaviors of  $v$  and  $D$  is obtained. Moreover, as we shall see in more detail in the next section, the fat-tailed time distribution promotes aging effects in which most physical properties strongly depend on the history of the sample [26, 27]. The  $\tau_p$  correlation is directly related to the spatial correlation, that decays abruptly with  $l_r$

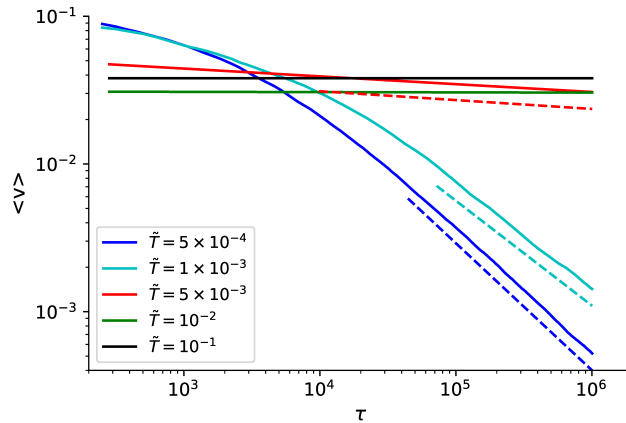


**Figure 3.** A log-log plot of the mean velocity versus the rescaled time, for the same parameters as those corresponding to Fig. 2. Dashed lines correspond to the asymptotic behavior and their slopes are stored in the third column of table 1. The slopes are equal to zero, for the curves in black and green colors, corresponding to a normal diffusion and a superdiffusive case. In order to minimize the effects of statistical fluctuations, the blue and cyan curves were calculated with  $\langle v \rangle = \langle z \rangle / \tau$  (see section 3.1).

(see Eq. (4)). Therefore,  $\tau_p$  is not correlated because we assume  $\lambda_p \gg l_r$ , i.e.  $\lambda \ll 1$  (see Eq. (7)).

The effect of the ratchet potential asymmetry on the movement of the particles plays a similar role as the temperature of the system. Indeed, when the asymmetry  $\mu$  increases, superdiffusive behavior is obtained at lower temperatures (see Table 1, in which exponents for two values of temperature and  $\mu = 0.5$  are shown for comparison purposes).

In order to complete this section, it should be mentioned that, for disorder correlation length much larger than the period of the ratchet potential, that is, negligible randomness, normal and superdiffusive behaviors are reached, but the subdiffusive regimes are lost. This has been previously studied in [23] for particles driven by a constant external force over a landscape consisting of a symmetric periodic potential with quenched disorder identical to Eq. (4).

**In brief, the system goes from a subdiffusive behavior to a normal diffusion, going before through a superdiffusive behavior, when the temperature, the ratchet potential asymmetry or quenched noise correlation length are increased.**

### 3.2. Aging in the transport on the corrugated ratchet potential

In equilibrated states and in steady states, physical properties do not change with time. In contrast, in aging systems, the time translation invariance is broken leading to time-dependent dynamics. The aging of the transport on the corrugated ratchet potential



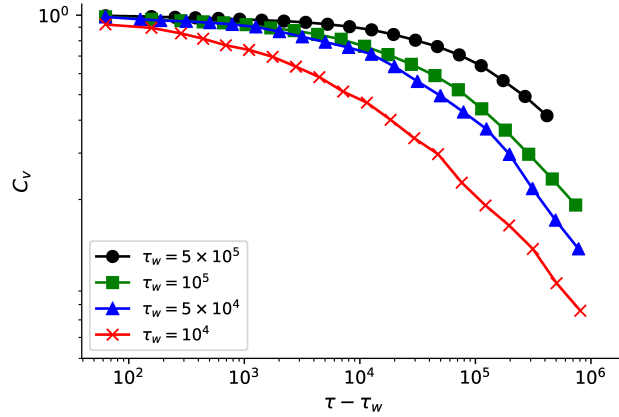


**Figure 4.** Two-time velocity correlation function  $C_v$  versus  $(\tau - \tau_w)$ , in log-log scale, corresponding to different choices of  $\tau_w$  as indicated and for the superdiffusive asymptotic case given by  $\tilde{T} = 10^{-3}$ ,  $\tilde{F}_0 = 1.47$ ,  $\lambda = 0.095$  and  $\mu = 0.5$  (see table 1). Here  $C_v$  was averaged over  $10^4$  samples and a temporal statistic average was also done.

can be measured through the two-time velocity correlation  $C_v(\tau, \tau_w)$  given by Eq. (9), with  $\tau_w$  the observation time or waiting time. Fig. 4 shows  $C_v$  as a function of  $(\tau - \tau_w)$ , corresponding to a asymptotic superdiffusive regime, for different  $\tau_w$ . The velocity correlation depends on the observation time  $\tau_w$ , which is the only relevant time scale for the dynamics of this transport. In addition, Fig. 4 shows that the older systems, with longer waiting time (circle and square symbols) relax in a slower manner than younger ones (triangle and cross symbols). This can be quantified, assuming that  $C_v$  depends on  $\tau/\tau_w^\chi$ , with  $0 < \chi \leq 1$ . Thus, we propose the scaling on the  $x$  axis given by  $(\tau - \tau_w)/\tau_w^\chi$ . Figs. 5 shows that the data from Fig. 4 can be fully collapsed by the previous scaling by taking  $\chi = 0.8$ .

**Note that, in this section, we use a ratchet potential asymmetry  $\mu = 0.5$  instead of 0.1 due only to a computational cost that grows with smaller asymmetries. In addition, more samples are required to calculate the velocity correlation function.**

In particular, the cases  $\chi < 1$  have been called subaging because the effective relaxation time grows more slowly than the age of the system [28, 29]. Indeed, the correlation function  $C_v$  is linearly related to the response to an external perturbation through generalized Fluctuation-Dissipation theorem [30]. According to this theorem, when the system is disturbed at time  $\tau_w$  by a sudden force, the relaxation time is  $\tau_w^\chi$ . Therefore, the system forgets the perturbation, after a time  $\tau_w^\chi$  less than its age  $\tau_w$ , provided  $\chi < 1$ .

The aging exponent depends on the way that particles explore the corrugated ratchet potential. Fig. 6 shows the two-time velocity correlation function  $C_v$  for an example of subdiffusive transport. Here the aging effect is less than that found for superdiffusive transport. In fact, a good collapse of data of Fig. 6 is obtained in Fig. 7,

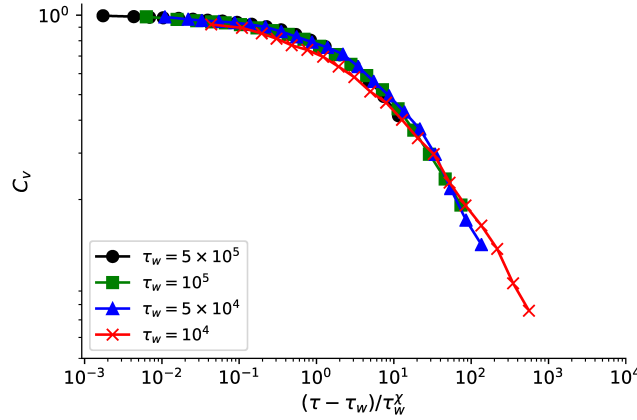


**Figure 5.** Scaling of the two-time velocity correlation function  $C_v$  versus  $(\tau - \tau_w)/\tau_w^\chi$ , obtained by setting  $\chi = 0.8$ , for the data shown in Fig. 4

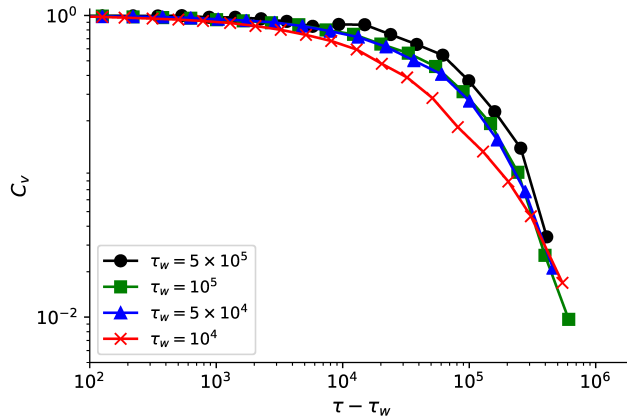


**Figure 6.** Two-time velocity correlation function  $C_v$  versus  $(\tau - \tau_w)$ , in log-log scale, corresponding to different choices of  $\tau_w$  as indicated and for the subdiffusive asymptotic case given by  $\tilde{T} = 3 \times 10^{-4}$ ,  $\tilde{F}_0 = 1.47$ ,  $\lambda = 0.095$  and  $\mu = 0.5$  (see table 1). Here  $C_v$  was averaged over  $10^3$  samples and a temporal statistic average was also done.

in which the x-axis is scaling as  $(\tau - \tau_w)/\tau_w^\chi$ , with  $\chi = 0.1$ . Regarding scaled figures 5 and 7, we want to point out that the quality of the scaled fits appears to be better for larger values of  $\tau_w$ .

Finally,  $\chi = 0$  is obtained for normal diffusion. Here  $C_v$  depends only on the time difference  $(\tau - \tau_w)$  and the system is not aging. In such case, the particles explore the whole phase space because of the presence of thermal fluctuations and the system is ergodic. For  $0 < \chi \leq 1$  the system is also ergodic but exhibits an extremely slow relaxation weakly breaking the ergodicity. For superdiffusive transports, the number of trapped particles that remain in that state grows slowly with time affecting collective motion. In contrast, for subdiffusive transports, most of the particles explore the traps

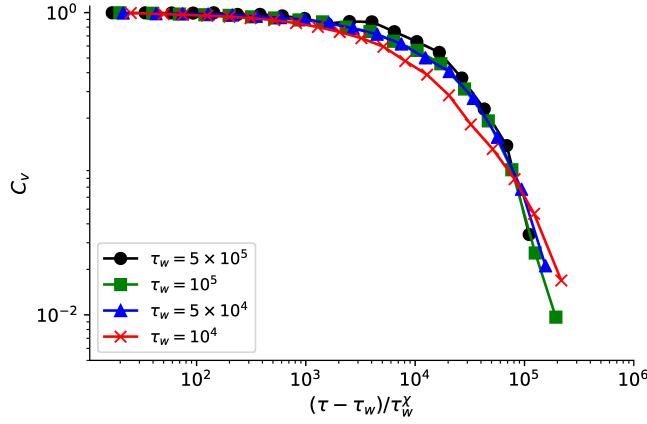


**Figure 7.** Scaling of the two-time velocity correlation function  $C_v$  versus  $(\tau - \tau_w)/\tau_w^\chi$ , obtained by setting  $\chi = 0.1$ , for the data shown in Fig. 6.

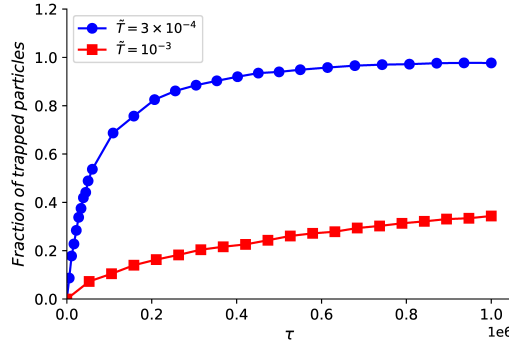


**Figure 8.** Fraction of trapped particles as a function of  $\tau$  in the superdiffusion (red square symbols) and in the subdiffusion (blue circle symbols). The parameters are the same as in Figs. 4 and 6, for the superdiffusive transport and subdiffusion transport, respectively. The fraction of trapped particles is significantly higher for the subdiffusive movement than for the superdiffusive movement.

and the system tends to ergodicity. This is clearly observed in Fig. 8, where the fraction of particles trapped in a potential well for a time period  $\tau_p$  as a function of  $\tau$  are shown for superdiffusive and subdiffusive transport respectively. Thus, aging related exponent  $\chi$  depends on the diffusion of particles on the corrugated ratchet potential.

#### 4. Conclusions

Anomalous diffusion and subaging appear in the motion of particles in a ratchet potential with both, correlated weak spatial disorder and thermal noise for different temperatures. The correlation of spatial disorder allows us to change the rugosity of the ratchet potential. This leads to different categories of diffusion at long times, as the temperature

of the system is varied: At high temperatures the particles undergo normal diffusion, whereas at intermediate temperatures we observe a superdiffusive motion and at low temperatures the motion becomes subdiffusive. In all cases, the mean velocity of the particles decreases with time or is at most constant, due to the interplay between the thermal noise and the landscape generated by the spatial disorder.

We find that the mean velocity has a power dependence on time that depends on the type of diffusion. We derived a relation (see Eq. (11)) between the asymptotic exponents of the mean velocity of the particles and those of the diffusion coefficient. In addition, we find that the system exhibits a behavior reminiscent to subaging and weak nonergodicity. When the details of the landscape do not affect the particle motion and a slowly growing fraction of particles remain trapped for long time, the dynamics becomes superdiffusive. This breaks the ergodicity because the time for the system to explore the whole phase space becomes enormously long [31]. We find subaging in superdiffusive transport. On the other hand, the system tends to recover its ergodicity in the subdiffusive case. These behavior were found after a superdiffusive transient due to a high quenched disorder and for an amplitude of the external force that is higher than the amplitude of the ratchet force. In contrast, a regular ratchet movement is found for an amplitude of the external force that is less than the amplitude of the ratchet force after a subdiffusive transient. In this case, a net motion is obtained for high enough temperatures that combined with the external force let the particle overcome both the ratchet potential and the quenched disorder.

In summary, we found a set of dramatic anomalous behaviors as diverse as subtransport, subdiffusion, and superdiffusion with subaging when the periodic ratchet potential is modified with a small amount of correlated weak disorder and thermal noise.

## 5. Bibliography

- [1] K. Binder, A. P. Young, Spin glasses: Experimental facts, theoretical concepts, and open questions, *Rev. Mod. Phys.* 58 (1986) 801–976.
- [2] J. Baran, N. A. Davydova, M. Drozd, Structural organizations in supercooled liquid 2-biphenylmethanol, *J. Mol. Liquids* 5127 (2006) 109–112.
- [3] C. C. Matthai, N. H. March, D. Lamoén, Supercooled molecular liquids and the glassy phases of chemically bonded n, p, as, si and ge, *Phys. and Chem. of Liquids* 47 (2009) 607–613.
- [4] C. Pelleta, M. Cloitre, The glass and jamming transitions of soft polyelectrolyte microgel suspensions, *Soft Matter* 12 (2016) 3710–3720.
- [5] M. Mézard, G. Parisi, M. Virasoro, Spin glass theory and beyond. World Scientific lecture notes in physics, World Scientific New York, 1987.
- [6] A. Cavagna, Supercooled liquids for pedestrians, *Physics Reports* 476 (2009) 51–124.
- [7] R. N. Zia, B. J. Landrum, W. B. Russel, A micro-mechanical study of coarsening and rheology of colloidal gels: Cage building, cage hopping, and smoluchowski’s ratchet, *J. Rheol.* 58 (5) (2014) 1121–1157.
- [8] P. Chaudhuri, L. Berthier, Ultra-long-range dynamic correlations in a microscopic model for aging gels, *Phys. Rev. E* 95 (2017) 060601(R).
- [9] B. Göbel, I. Mertig, Skyrmion ratchet propagation: utilizing the skyrmion hall effect in ac racetrack storage devices, *Sci. Rep.* 11 (2021) 3020.

- [10] S. S. P. Parkin, M. Hayashi, L. Thomas, Magnetic domain-wall racetrack memory., *Science* 320 (2008) 190–194.
- [11] F. Jonietz, et al, Spin transfer torques in mnsi at ultralow current densities, *Science* 330 (2010) 1648–1651.
- [12] I. E. Dzyaloshinskii, Theory of helicoidal structures in antiferromagnets, I. Nonmetals *Sov. Phys. JETP* 19 (1964) 960.
- [13] A. N. Bogdanov, New localized solutions of the nonlinear field equations, *JETP Letters* 62 (1995) 247.
- [14] A. N. Bogdanov, U. K. Rossler, Chiral symmetry breaking in magnetic thin films and multilayers, *Phys. Rev. Lett.* 87 (2001) 037203.
- [15] A. Fert, N. Reyren, V. Cros, Magnetic skyrmions: advances in physics and potential applications, *Nat. Rev. Mater.* 2 (2017) 17031.
- [16] C. Reichhardt, D. Ray, C. J. O. Reichhardt, Collective transport properties of driven skyrmions with random disorder, *Phys. Rev. Lett.* 114 (2015) 217202.
- [17] L. B. Brown, U. C. Täuber, M. Pleimling, The effect of the magnus force on skyrmion relaxation dynamics, *Phys. Rev. B* 97 (2018) 020405(R).
- [18] X. Zhang, et al, Skyrmion-electronics: Writing, deleting, reading and processing magnetic skyrmions toward spintronic applications, *Phys. Rev. B* 100 (2019) 024410.
- [19] E. Vincent, J. Hammann, M. Ocio, J. P. Bouchaud, L. F. Cugliandolo, Vol. 492 of *Lecture Notes in Physics*, Springer, New York, 1997, pp. 184–219.
- [20] M. Picco, F. Ricci-Tersenghi, F. Ritort, Aging effects and dynamic scaling in the 3d edwards-anderson spin glasses: a comparison with experiments, *Eur Phys J B* 21 (2001) 211–217.
- [21] K. I. Mazzitello, D. G. Zarlenga, C. M. Arizmendi, Anomalous transport on a corrugated ratchet potential, *J. Phys.: Conf. Ser.* 1978 (2021) 012017.
- [22] R. Bartussek, P. Hänggi, J. G. Kissner, Periodically rocked thermal ratchets, *Europhys. Lett.* 28 (1994) 459–464.
- [23] M. Khoury, A. M. Lacasta, J. M. Sancho, K. Lindenberg, Weak disorder: Anomalous transport and diffusion are normal yet again, *Phys. Rev. Lett.* 106 (2011) 090602.
- [24] D. G. Zarlenga, G. L. Frontini, F. Family, C. M. Arizmendi, Transient superdiffusive motion on a disordered ratchet potential, *Physica A* 523 (2019) 172 – 179.
- [25] I. Goychuk, T. Pöschel, Anomalous diffusion in disordered media: statistical mechanics, models and physical applications, *Phys. Rep.* 195 (4–5) (1990) 127–293.
- [26] E. Vincent, J. Hammann, M. Ocio, singapore Edition, World Scientific Pub. Co. Pte. Ltd, 1992, p. 207.
- [27] L. C. E. Struick, *Physical Aging in Amorphous Polymers and Other Materials*, Elsevier, Houston, 1978.
- [28] B. Rinn, P. Maass, J.-P. Bouchaud, Multiple scaling regimes in simple aging models, *Phys. Rev. Lett.* 84 (23) (2000) 5403–5406.
- [29] J.-P. Bouchaud, L. Cugliandolo, J. Kurchan, M. Mézard, in *Spin-glasses and Random Fields*, World Scientific, Singapore, 1998.
- [30] A. Sarracino, A. Vulpiani, On the fluctuation-dissipation relation in non-equilibrium and non-hamiltonian systems, *Chaos* 29 (8) (2019) 083132.
- [31] J. Spiechowicz, J. Luczka, P. Hänggi, Transient anomalous diffusion in periodic systems: ergodicity, symmetry breaking and velocity relaxation, *Sci. Rep.* 6 (2016) 30948.